

Accelerated Motion Correction for MRI using Score-Based Generative Models

Brett Levac[†] Ajil Jalal* Jonathan I. Tamir[†]

[†] University of Texas, Austin, ECE

*University of California, Berkeley, EECS

Abstract

Magnetic Resonance Imaging (MRI) is a powerful medical imaging modality, but unfortunately suffers from long scan times which, aside from increasing operational costs, can lead to image artifacts due to patient motion. Motion during the acquisition leads to inconsistencies in measured data that manifest as blurring and ghosting if unaccounted for in the image reconstruction process. Various deep learning based reconstruction techniques have been proposed which decrease scan time by reducing the number of measurements needed for a high fidelity reconstructed image. Additionally, deep learning has been used to correct motion using end-to-end techniques. This, however, increases susceptibility to distribution shifts at test time (sampling pattern, motion level). In this work we propose a framework for jointly reconstructing highly sub-sampled MRI data while estimating patient motion using score-based generative models. Our method does not make specific assumptions on the sampling trajectory or motion pattern at training time and thus can be flexibly applied to various types of measurement models and patient motion. We demonstrate our framework on retrospectively accelerated 2D brain MRI corrupted by rigid motion.

Keywords: Magnetic Resonance Imaging (MRI), Motion Correction, Accelerated Reconstruction, Joint Estimation, Score Models, Generative Models

1 Introduction

MRI is a powerful medical imaging modality that boasts superior soft tissue contrast which can be leveraged to diagnose a variety of adverse health conditions. Compared to other medical imaging methods, however, MRI is relatively slow. Many previous works have developed methods to decrease the data requirements for solving the ill-posed inverse problem of sub-sampled image reconstruction [1, 2], including through deep learning [3–7]. Even with sub-sampling, MRI is highly susceptible to patient motion [8], which leads to inconsistencies in measurement data at the time of reconstruction. The image degradation due to motion-corrupt data can manifest as blurring or ghosting which possibly render the image nondiagnostic, and often necessitates reacquiring the scan. It has been reported that on average motion corrupted scans in a pediatric setting have led some hospitals to incur nearly \$365K in additional costs each year due to motion artifacts [9].

Many approaches to address motion have been proposed, including prospective methods used at scan time like hard and soft gating. These methods measure motion during the scan using motion navigators [10] or external measurement devices such as respiratory bellows, nuclear magnetic resonance probes, and optical tracking. While powerful, these approaches require modification to the pulse sequence or additional hardware and can ultimately increase scan time. Alternative approaches, which are considered retrospective methods, incorporate the motion into the MRI forward model and solve a modified reconstruction problem after the scan has been completed [11–13].

Recent developments in deep learning have allowed for end-to-end supervised training methods in which a neural network (NN) is used to map motion corrupt inputs to (ideally) motion free outputs [14]. These techniques have shown great promise, however, recent work has displayed that the network’s performance at test time is highly dependent on the motion simulation parameters used at training time [15]. More recently,

supervised learning has been used as one step in a larger iterative algorithm that jointly solves for the image and the motion parameters [16]. These methods have primarily been applied to the low acceleration regime, and may still suffer from overfitting to the specific motion simulation at training time.

In parallel, promising recent work in deep learning based image reconstruction has used generative modeling to learn image priors separate from the measurement forward model [5, 17]. By explicitly decoupling the forward model and the image prior, generative model based techniques have an increased robustness to test time shifts in the forward operator such as sampling trajectory [5]. As a result, the reconstruction can flexibly handle other modifications to the forward model without retraining the generative prior.

The aim of this work is to extend recent advances in generative models to a joint estimation technique which can correct motion at high acceleration rates by leveraging recent advances in score models for inverse problems and their robustness to forward model shifts. We study the utility of our method in reconstructing retrospectively sub-sampled multi-coil brain MRI corrupted by simulated rigid motion.

2 Methods

2.1 Image Formation and Motion Simulation

We restrict our experiments to correcting in-plane, rigid body motion which is a common assumption for motion correction techniques applied to brain imaging [12, 13, 16]. It is known from basic Fourier theory that translations in image space result in linear phase shifts in the Fourier domain (k-space), while rotations in image space result in rotations in k-space. This allows us to model patient motion as an alteration to the motion-free MRI forward operator. The multi-coil MRI forward model with motion admits the following form:

$$y = L_\phi N_{R_\theta K} Sx + w, w \sim \mathcal{N}(0, \sigma^2 I). \quad (1)$$

Here $x \in \mathbb{C}^N$ is the motion-free image, $S \in \mathbb{C}^{NC \times N}$ contains the C coil sensitivity maps, $y \in \mathbb{C}^{MC}$ is the corrupted k-space measurements, R_θ denotes a set of rotation matrices for each motion state angle (θ) observed during the acquisition, L_ϕ is a diagonal matrix which applies linear phase shifts to acquired k-space depending upon the object’s translation (ϕ) observed during acquisition, K defines a set of k-space coordinates which are the intended trajectory of the acquisition, and $N_{R_\theta K}$ is a linear function of the image x which takes the Non-uniform Fast Fourier Transform (NUFFT) of Sx at the coordinates $R_\theta K$. Here we see that rotations in image space are implemented by rotation of the corresponding coordinates in the NUFFT, while translations are implemented with the corresponding phase shift in k-space. For the remainder of this paper we will denote the forward operation as:

$$y = A_\kappa x + w, w \sim \mathcal{N}(0, \sigma^2) \quad (2)$$

where A_κ includes the NUFFT and coil map weighting while it also implicitly capturing all rotation and translation effects, at all times throughout the scan, in κ . Our goal is to jointly estimate x and κ . We note that y is a linear function of x but is non-linear in κ . This means that finding a global solution, even in the fully sampled case, is not guaranteed due to the non-convexity introduced by estimating κ .

Additionally, for the remainder of the paper we make the assumption, both when simulating and estimating motion, that k-space points acquired in the same repetition time (TR) are assumed to have the same motion state. This assumption is well supported as in common sequences like fast spin echo (FSE), timing between phase encode (PE) lines in a single echo train are on the order of milliseconds while points in different TRs are separated on the order of seconds [15]. In particular a fully sampled scan in our simulations has 384×384 k-space points and we choose our (fully sampled) sequence to have an echo train length (ETL) of 8 and 48 TRs. We therefore simulate 48 different angles, x-translations, and y-translations in the fully sampled case. In all experiments, scan acceleration (R) is applied along the TR dimension. For example, this means that for $R = 4$, $ETL = 8$ and $TRs = 12$ resulting in the simulation and estimation of 12 different motion states, corresponding to a 4x faster scan. We note that modeling motion across TRs is not strictly necessary, and in addition the model can be extended to non-rigid motion by modifying the forward operator to include a parameterized deformation field which can not be easily included in the description of the NUFFT. In this case the motion state is expanded from three parameters to a larger basis set.

2.2 Score Models

Recent work in deep learning has led to impressive progress in the area of generative modeling [18,19], and in particular, score-based generative models [17]. Given i.i.d. training samples drawn from a high-dimensional probability density p , score-based generative models can estimate the *score* of p , defined as $\nabla_x \log p(x)$, by training a NN via denoising score matching [17]. These models can produce new samples from p by initializing $x_0 \sim \mathcal{N}(0, I_N)$, and running annealed Langevin dynamics for T steps:

$$x_{t+1} = x_t + \eta_t \nabla \log p(x_t) + z_t, \tag{3}$$

where $z_t \sim \mathcal{N}(0, 2\eta_t I_N)$ is i.i.d. Gaussian. As $\eta_t \rightarrow 0, T \rightarrow \infty$, the distribution of x_T converges to p [17].

If we know the distribution of $y|x$, Eqn (3) can be modified using Bayes’ rule to sample from the *posterior distribution* $p(x|y)$, and this procedure has been successful in inverse problems such as compressed sensing MRI. We emphasize that during training, the score model is agnostic to the MRI forward model, which enhances its robustness to forward model shifts when applied to inverse problems [5].

2.3 Score-Based Accelerated Motion Correction

As stated above, prior works have shown positive results when using score models to solve ill-posed inverse problems like sub-sampled image reconstruction [5–7]. In prior work, however, the forward model is assumed to be fixed and known throughout the reconstruction procedure. In our work, however, we assume that our forward operator A_κ belongs to a restricted class of operators with unknown parameters κ which must be learned during the inference. Another way of viewing this problem is as posterior sampling from the joint distribution $p(x, \kappa|y)$. Under this joint posterior, we arrive at the following update equations:

$$x_{t+1} = x_t + \eta_t \nabla_{x_t} \log p(x_t, \kappa_t|y) + z_t, \tag{4}$$

$$\kappa_{t+1} = \kappa_t + \lambda_t \nabla_{\kappa_t} \log p(x_t, \kappa_t|y) + \xi_t, \tag{5}$$

where $z_t \sim \mathcal{N}(0, 2\eta_t I), \xi_t \sim \mathcal{N}(0, 2\lambda_t I)$ are i.i.d. Gaussian.

We assume independence between x and κ and use Bayes’ rule to further simplify the update equations to

$$x_{t+1} = x_t + \eta_t \nabla_{x_t} (\log p(y|x_t, \kappa_t) + \log p(x_t)) + z_t, \tag{6}$$

$$\kappa_{t+1} = \kappa_t + \lambda_t \nabla_{\kappa_t} (\log p(y|x_t, \kappa_t) + \log q(\kappa_t)) + \xi_t. \tag{7}$$

Inserting the likelihood function given by the forward model in Eqn (2) we get the following final update steps:

$$x_{t+1} = x_t + \eta_t \left(\frac{A_{\kappa_t}^H (y - A_{\kappa_t} x_t)}{\sigma^2} + f(x_t) \right) + z_t, \tag{8}$$

$$\kappa_{t+1} = \kappa_t + \lambda_t \nabla_{\kappa_t} (\|y - A_{\kappa_t} x\|_2^2 + \log q(\kappa_t)) + \xi_t, \tag{9}$$

where $f(x_t)$ is the score-model trained to estimate $\nabla \log p(x)$. We note that this formulation allows for the incorporation of different priors over the motion parameters κ .

2.4 Implementation Details

The score model (f) in Eq. (8) was trained on 14,539 T2-weighted brain images from the fastMRI dataset [20]. Sensitivity maps were estimated using ESPIRiT [21]. Simulated ground truth motion states (κ_{GT}) were chosen as $\kappa_{GT} \sim U(-2, 2)$ i.i.d. for each TR. This level was chosen based off the severity of the resulting artifacts which visually matched motion-corrupt data from prior work [14] and led to nondiagnostic image quality even at low accelerations. The prior over motion parameters used in our score update steps was $\kappa \sim U(-15, 15)$ so as not to assume perfect knowledge over the prior distribution which generated the motion parameters.

Although the use of the NUFFT operator in our forward model allows for any non-Cartesian sampling trajectory, the results we present here are for Cartesian trajectories with equispaced sub-sampling (Fig. 1).

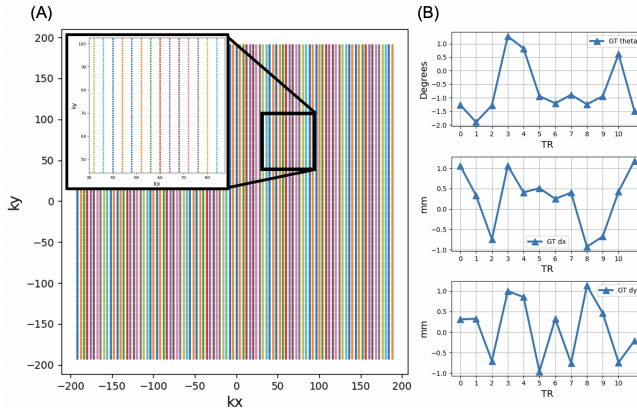


Figure 1: (a) $R = 4$ Sampling trajectory where each color denotes a separate TR. 12 TRs total each having ETL=8. (b) corresponding motion simulation (rotation, translation) for each TR (12 motion states in total).

We compared our method to two different L1-wavelet [2] reconstructions, implemented using BART [22], where (1) uses motion corrupt data and (2) uses motion free data. For prior methods which rely on SENSE based schemes [1] for the final reconstruction [12, 13, 16] (1) represents the worst case scenario while (2) represents the best case scenario. Our method, however, jointly estimated motion parameters and the image. We performed experiments on 11 validation slices and 39 test slices from the T2-weighted brain fastMRI dataset at retrospective acceleration factors of ($R = 4, 4.8, 6$). Each slice was independently corrupted by motion and additive Gaussian noise.

All reconstruction hyperparameters for the three methods were tuned on the validation set and held fixed on the test set. Normalized root mean squared error (NRMSE) was used to evaluate the performance of the methods. Our algorithm was implemented in PyTorch and gradients for κ_t in Eq. (9) were calculated through auto-differentiation. Inference was run on one Nvidia RTX 3090. As all training, validation, and test data was taken from a publicly available dataset [20] and motion was retrospectively simulated, ethical approval was not required.

3 Results

Quantitative NRMSE metrics are shown for each method in Table 1 at accelerations of ($R = 4, 4.8, 6$). Our reconstruction often converges to motion estimates with an offset from the ground-truth due to the ambiguity between two data-consistent reconstructions with a fixed motion offset. We therefore align our reconstructions to the motion-free ground-truth before evaluating NRMSE. Example reconstructions for $R = 4.8$ and $R = 6$ are shown in Fig. 3. We visualize in Fig. 2 the intermediate reconstruction images along with the estimated motion trajectories at various points during inference.

Table 1: Reconstruction NRMSE averaged over the test set.

| | R= 4 | R= 4.8 | R= 6 |
|---------------------------|--------------|--------------|--------------|
| L1 Wavelet Motion Corrupt | 0.343 | 0.345 | 0.363 |
| L1 Wavelet Motion Free | 0.092 | 0.115 | 0.158 |
| Ours | 0.090 | 0.104 | 0.145 |

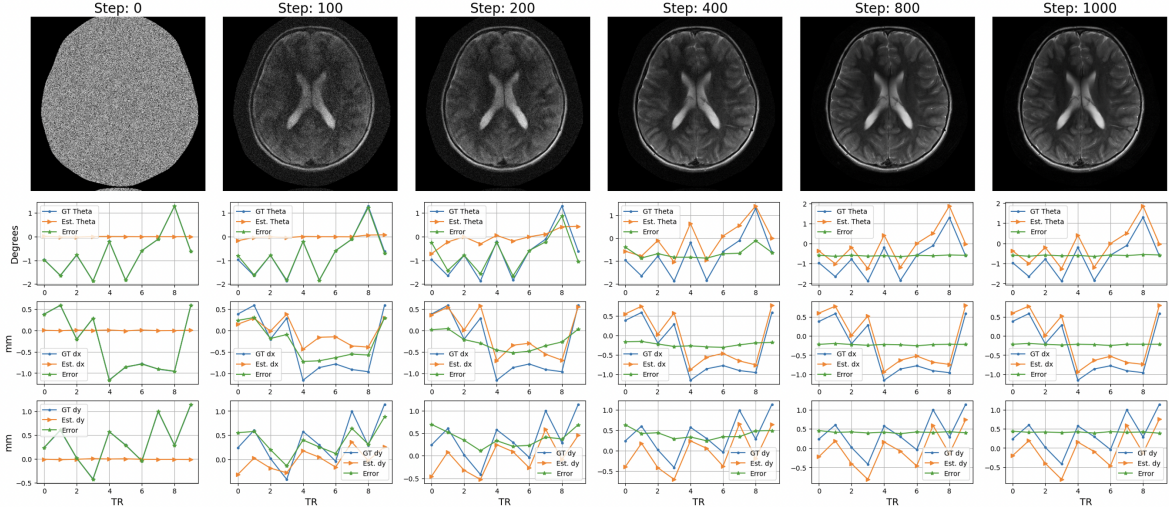


Figure 2: **(Top)** Image progression as inference proceeds. **(Bottom)** Motion estimation (rotation, x-translation, y-translation) as inference proceeds. In both figures each *Step* indicates a different noise level in the Langevin sampling inference.

4 Discussion

From our results we see that, *even with no motion*, L1-wavelet based reconstruction methods hit a performance limit at high 2D acceleration factors, in agreement with previously reported literature [3–5]. In contrast, our method, *which was blind to the motion*, is able to both estimate the motion trajectories while also reconstructing a sub-sampled image with high fidelity (Fig. 3). Although the performance of score models in the presence of corrupted forward operators has not been displayed previously, we showed that by viewing the inference procedure as posterior sampling jointly over the image and motion parameters we can achieve high fidelity motion correction at large acceleration rates for retrospectively corrupted data.

We note that the training and inference processes for solving inverse problems with score models are unique when compared to end-to-end supervised methods. Score models are trained only on ground-truth images which, in part, makes the inference process agnostic to shifts in sampling pattern, and motion distribution. On the other hand, end-to-end methods are known to degrade when the test time distributions do not align with the training distributions, which would potentially require re-training for different motion corruption [15]. Although we only simulated and estimated one motion state per TR, this can be relaxed to estimate motion states for every PE at the cost of larger computational burden. However, assuming that motion occurs only between PEs neglects higher order effects like magnetization history which is left for future work.

5 Conclusion

Our proposed method of jointly optimizing motion-corrupt MRI with score-based generative models provides high fidelity images compared to even the best case scenario (motion free measurements) for L1 Wavelet, which is similar to previously proposed joint motion correction techniques [12,13,16] but at higher acceleration levels. This retrospective study, however, did not compare to end-to-end supervised methods which are becoming popular motion correction techniques [14], but are also not typically not used at high accelerations, nor was it applied to prospectively acquired motion-corrupt MRI.

6 Acknowledgments

This work was supported by NSF IFML 2019844, NIH U24EB029240, and Oracle for Research Fellowship.

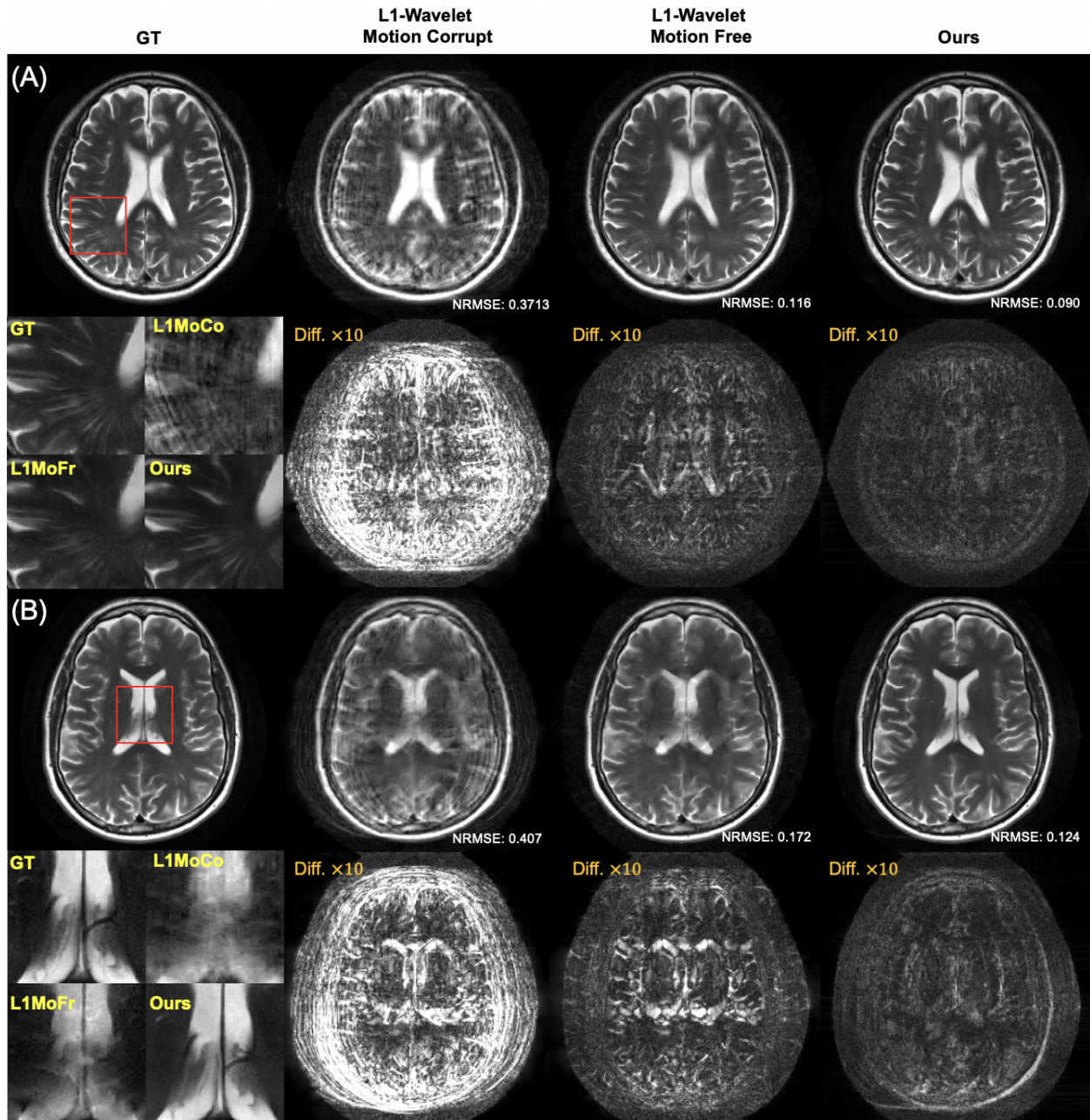


Figure 3: Reconstruction results for L1 Wavelet (with and without motion) and our method for (A) $R = 4.8$, and (B) $R = 6$ acceleration factors.

References

- [1] Klaas P. Pruessmann, Markus Weiger, Markus B. Scheidegger, and Peter Boesiger, “Sense: Sensitivity encoding for fast mri,” *Magnetic Resonance in Medicine*, vol. 42, no. 5, pp. 952–962, 1999.
- [2] Michael Lustig, David Donoho, and John M Pauly, “Sparse mri: The application of compressed sensing for rapid mr imaging,” *Magnetic Resonance in Medicine: An Official Journal of the International Society for Magnetic Resonance in Medicine*, vol. 58, no. 6, pp. 1182–1195, 2007.

- [3] Kerstin Hammernik, Teresa Klatzer, Erich Kobler, Michael P. Recht, Daniel K. Sodickson, Thomas Pock, and Florian Knoll, “Learning a variational network for reconstruction of accelerated mri data,” *Magnetic Resonance in Medicine*, vol. 79, no. 6, pp. 3055–3071, 2018.
- [4] Hemant K. Aggarwal, Merry P. Mani, and Mathews Jacob, “Modl: Model-based deep learning architecture for inverse problems,” *IEEE Transactions on Medical Imaging*, vol. 38, no. 2, pp. 394–405, 2019.
- [5] Ajil Jalal, Marius Arvinte, Giannis Daras, Eric Price, Alexandros G Dimakis, and Jonathan I Tamir, “Robust compressed sensing mri with deep generative priors,” *Advances in Neural Information Processing Systems*, 2021.
- [6] Guanxiong Luo, Martin Heide, and Martin Uecker, “MRI reconstruction via data driven markov chain with joint uncertainty estimation,” *arXiv preprint arXiv:2202.01479*, 2022.
- [7] Hyungjin Chung and Jong Chul Ye, “Score-based diffusion models for accelerated mri,” *Medical Image Analysis*, vol. 80, pp. 102479, 2022.
- [8] Maxim Zaitsev, Julian Maclaren, and Michael Herbst, “Motion artifacts in mri: A complex problem with many partial solutions,” *Journal of Magnetic Resonance Imaging*, vol. 42, no. 4, pp. 887–901, 2015.
- [9] Jakob M Slipsager, Stefan L Glimberg, Jes Sogaard, Rasmus R Paulsen, Helle H Johannesen, Pernille C Martens, Alka Seth, Lisbeth Marnner, Otto M Henriksen, Oline V Olesen, et al., “Quantifying the financial savings of motion correction in brain mri: a model-based estimate of the costs arising from patient head motion and potential savings from implementation of motion correction,” *Journal of Magnetic Resonance Imaging*, vol. 52, no. 3, pp. 731–738, 2020.
- [10] Joseph Y. Cheng, Tao Zhang, Nichanan Ruangwattanapaisarn, Marcus T. Alley, Martin Uecker, John M. Pauly, Michael Lustig, and Shreyas S. Vasanawala, “Free-breathing pediatric mri with nonrigid motion correction and acceleration,” *Journal of Magnetic Resonance Imaging*, vol. 42, no. 2, pp. 407–420, 2015.
- [11] Sajan Goud Lingala, Edward DiBella, and Mathews Jacob, “Deformation corrected compressed sensing (dc-cs): A novel framework for accelerated dynamic mri,” *IEEE Transactions on Medical Imaging*, vol. 34, no. 1, pp. 72–85, 2015.
- [12] Lucilio Cordero-Grande, Rui Pedro A. G. Teixeira, Emer J. Hughes, Jana Hutter, Anthony N. Price, and Joseph V. Hajnal, “Sensitivity encoding for aligned multishot magnetic resonance reconstruction,” *IEEE Transactions on Computational Imaging*, vol. 2, no. 3, pp. 266–280, 2016.
- [13] Melissa W Haskell, Stephen F Cauley, and Lawrence L Wald, “Targeted motion estimation and reduction (TAMER): data consistency based motion mitigation for mri using a reduced model joint optimization,” *IEEE transactions on medical imaging*, vol. 37, no. 5, pp. 1253–1265, 2018.
- [14] Patricia M Johnson and Maria Drangova, “Conditional generative adversarial network for 3d rigid-body motion correction in mri,” *Magnetic Resonance in Medicine*, vol. 82, no. 3, pp. 901–910, 2019.
- [15] Brett Levac, Sidharth Kumar, Sofia Kardonik, and Jonathan I. Tamir, “Fse compensated motion correction for mri using data driven methods,” in *Medical Image Computing and Computer Assisted Intervention – MICCAI 2022*, Cham, 2022, pp. 707–716, Springer Nature Switzerland.
- [16] Melissa W Haskell, Stephen F Cauley, Berkin Bilgic, Julian Hossbach, Daniel N Splitthoff, Josef Pfeuffer, Kawin Setsompop, and Lawrence L Wald, “Network accelerated motion estimation and reduction (NAMER): convolutional neural network guided retrospective motion correction using a separable motion model,” *Magnetic resonance in medicine*, vol. 82, no. 4, pp. 1452–1461, 2019.
- [17] Yang Song and Stefano Ermon, “Generative modeling by estimating gradients of the data distribution,” *Advances in Neural Information Processing Systems*, pp. 11918–11930, 2019.

- [18] Ian Goodfellow, Jean Pouget-Abadie, Mehdi Mirza, Bing Xu, David Warde-Farley, Sherjil Ozair, Aaron Courville, and Yoshua Bengio, “Generative adversarial networks,” *Communications of the ACM*, vol. 63, no. 11, pp. 139–144, 2020.
- [19] Diederik P Kingma and Max Welling, “Auto-encoding variational bayes,” *arXiv preprint arXiv:1312.6114*, 2013.
- [20] Florian Knoll, Jure Zbontar, Anuroop Sriram, Matthew J Muckley, Mary Bruno, Aaron Defazio, Marc Parente, Krzysztof J Geras, Joe Katsnelson, Hersh Chandarana, et al., “fastmri: A publicly available raw k-space and dicom dataset of knee images for accelerated mr image reconstruction using machine learning,” *Radiology. Artificial intelligence*, vol. 2, no. 1, 2020.
- [21] Martin Uecker, Peng Lai, Mark J. Murphy, Patrick Virtue, Michael Elad, John M. Pauly, Shreyas S. Vasanawala, and Michael Lustig, “Espirit—an eigenvalue approach to autocalibrating parallel mri: Where sense meets grappa,” *Magnetic Resonance in Medicine*, vol. 71, no. 3, pp. 990–1001, 2014.
- [22] Martin Uecker, Jonathan I Tamir, Frank Ong, and Michael Lustig, “The bart toolbox for computational magnetic resonance imaging,” in *Proc Intl Soc Magn Reson Med*, 2016, vol. 24.